

КРАТКИЕ СООБЩЕНИЯ

UDC 541.67:547.13:546.73

CRYSTAL STRUCTURE AND MAGNETIC PROPERTIES OF HYBRID MATERIALS SELF-ASSEMBLY FROM TETRA(ISOTHIOCYANATE)COBALT(II) ANION AND TRISUBSTITUTED BENZYLTRIPHENYLPHOSPHINIUM

S.-L. Dai, Z.-P. Cheng, R.-K. Huang, Q.-Y. Guan, Y.-J. Liang,
W.-Q. Huang, J.-R. Zhou, C.-L. Ni*Department of Applied Chemistry, College of Science, Institute of Biomaterials, South China Agricultural University, Guangzhou, P. R. China*

E-mail: niclchem@scau.edu.cn (C.-L. Ni)

Received October, 7, 2012

Revised — November, 16, 2012

A new hybrid material $[\text{BiF4BrBzTPP}]_2[\text{Co}(\text{NCS})_4]$ (**1**) ($\text{BiF4BrBzTPP}^+ = 2,6\text{-bisfluoro-4-bromobenzyltriphenylphosphinium}$, $\text{NCS}^- = \text{isothiocyanate}$) is synthesized and characterized by elemental analyses, IR, UV spectra, ESI-MS, molar conductivity, single crystal X-ray diffraction and magnetic susceptibility measurements. Compound **1** crystallizes in the monoclinic space group $C2/c$ with $a = 15.272(2) \text{ \AA}$, $b = 24.779(3) \text{ \AA}$, $c = 14.482(2) \text{ \AA}$, $\beta = 101.037(2)$, $V = 5378.9(12) \text{ \AA}^3$, $Z = 4$. The compound comprises two cations and one anion which exhibits a distorted tetrahedral coordination geometry. The short $\text{F}\cdots\text{F}$, $\text{C}\cdots\text{Br}$ and $\text{N}\cdots\text{Br}$ interactions and $\text{C}-\text{H}\cdots\text{S}$ hydrogen bonds consolidate the stacking of the molecules. Magnetic susceptibility measurements in the temperature range 2–300 K show that **1** exhibits weak antiferromagnetic coupling behavior.

Keywords: tetra(isothiocyanate)cobalt(II) anion, substituted benzyl triphenylphosphinium, crystal structure, magnetic properties.

Hexacyanometalate anions of transition metals $[\text{M}(\text{CN})_6]^{n-}$ and the tetra(isothiocyanato)cobaltate anion $[\text{Co}(\text{NCS})_4]^{2-}$ as building blocks have been widely utilized in the design of new hybrid materials [1–4]. The nature and geometry of the counter cations strongly affect the stacking structure of the anions and, hence, the properties of the hybrid materials. The substituted benzyltriphenylphosphinium derivatives, abbreviated as $([\text{RBzTPP}]^+)$ ($\text{R} = \text{H}, \text{F}, \text{Cl}, \text{CN}, \text{NO}_2$; $\text{TPP} = \text{triphenylphosphine}$), as multifunctional cations of $[\text{M}(\text{mnt})_2]^{n-}$ ($\text{M} = \text{Ni}^{3+}, \text{Cu}^{2+}$; $n = 1$ or 2) anions have developed a new series of magnetic materials [5–8], and the change in the substituted group in the phenyl ring of the benzyl group of the cations affects the stacking mode of $[\text{M}(\text{mnt})_2]^{n-}$ anions and the magnetic properties of these hybrid materials. Recently, in order to broaden our research, we have used $[\text{RBzTPP}]^+$ as counter cations of the $[\text{Co}(\text{NCS})_4]^{2-}$ anion and obtained two new hybrid materials whose magnetic properties have been investigated [9]. Based on these findings, we firstly synthesized a new hybrid material containing tri-substituted benzyltriphenylphosphinium $[\text{BiF4BrBzTPP}]_2[\text{Co}(\text{NCS})_4]$ (**1**) ($[\text{BiF4BrBzTPP}]^+ = 2,6\text{-bisfluoro-4-bromobenzyltriphenylphosphinium}$), and its crystal structure, weak interactions, the stacking mode and magnetic properties have been systematically investigated via elemental analyses, IR, UV spectra, X-ray diffraction and magnetic susceptibility measurements.

Experimental. Synthesis of $[\text{BiF4BrBzTPP}]_2[\text{Co}(\text{NCS})_4]$ (1**).** A methanol solution (20 cm^3) of KSCN (389 mg, 4 mmol) was added to a methanol solution (20 cm^3) of CoCl_2 (130 mg, 1 mmol) and the mixture was stirred for half an hour. Then a methanol solution (30 cm^3) of $[\text{BiF4BrBzTPP}]\text{Br}$ (1096 mg, 2 mmol) was added dropwise, and the mixture was allowed to stir for 2 h; then the blue fil-

trate was washed with cool ether and dried. Yield: 1006 mg, 81.9 %. All reagents used in the syntheses were purchased from commercial sources and used as received. [BiF₄BrBzTPP]Br was prepared by the literature procedure [10]. Elemental analyses for C, H, N were performed on a Model 240 Perkin Elmer CHN analytical instrument. IR spectra with KBr pellets were obtained with a IF66V FT-IR (400–4000 cm⁻¹) spectrophotometer. Electronic spectrum was recorded on a SHIMADZU UV-4000 spectrophotometer. The electrospray mass spectra [ESI-MS] were measured on a Finnigan LCQ mass spectrograph and the sample concentrations were 1.0 × 10⁻⁵ mol · l⁻¹. Molar conductivity was measured on a DDS-11A conductivity instrument using a platinum electrode. Magnetic susceptibility data for a crushed polycrystalline sample of the compound were collected over the temperature range of 2.0–300 K using a SQUID MPMS-XL magnetometer. *Anal. Calc.* For C₅₄H₃₈F₄Br₂N₄P₂CoS₄: C, 52.82; H, 3.12, N, 4.56, S, 10.45 %. Found: C, 52.77; H, 3.25, N, 4.51, S, 10.52 %. ESI-MS (CH₃CN): 468.2.

Single crystal XRD. The blue single crystals suitable for the X-ray structure analysis were obtained by evaporating the solution of **1** in MeOH for about two weeks, and measurements of the studied complexes were performed on a Smart APEX CCD area detector using graphite-monochromated MoK_α radiation ($\lambda = 0.71073 \text{ \AA}$) by the ω scan mode. The structures were solved by direct methods and refined on F^2 by full-matrix least-squares, employing Bruker's SHELXTL [11]. All non-hydrogen atoms were refined with anisotropic thermal parameters. All H atoms were placed in calculated positions, assigned fixed isotropic displacement parameters (1.2 times the equivalent isotropic U value of the attached atom), and allowed to ride on their respective parent atoms. The CIF file with complete information about the structure was deposited at CCDC (No. 904122), from which it is available free of charge on request at www.ccdc.cam.ac.uk/data_request/cif. Selected bond lengths and bond angles are listed in Table 1.

Main crystallographic parameters and characteristics of the X-ray diffraction experiment for **1**: C₅₄H₃₈F₄Br₂N₄P₂CoS₄; $FW = 1227.81$; monoclinic, $C2/c$; $a = 15.272(2)$, $b = 24.779(3)$, $c = 14.4817(19) \text{ \AA}$, $\beta = 14.4817(19)^\circ$, $V = 5378.9(12) \text{ \AA}^3$; $Z = 4$, $D_c = 1.516 \text{ g/cm}^3$; $\mu = 2.074 \text{ mm}^{-1}$; $1.6 < \theta < 25.0^\circ$; 19133 collected, 4739 unique, $R_{int} = 0.035$; GOOF = 1.030; R indices for $I > \sigma$ $R_1 = 0.0563$, $wR_2 = 0.1717$; R indices (all data) $R_1 = 0.0813$, $wR_2 = 0.1877$; residual electron density (max/min) = 0.40/−0.90 e/Å.

Table 1

Selected bond lengths (d , Å) and bond angles (ω , deg.) for **1**

Bond	d	Bond	d	Bond	d
Co(1)—N(1)	1.979(5)	S(1)—C(1)	1.624(6)	P(1)—C(21)	1.798(5)
Co(1)—N(2)	1.977(5)	S(2)—C(2)	1.633(5)	P(1)—C(27)	1.794(5)
N(1)—C(1)	1.143(7)	P(1)—C(9)	1.824(5)	F(1)—C(7)	1.524(7)
N(2)—C(2)	1.143(7)	P(1)—C(15)	1.806(5)	F(2)—C(3)	1.498(7)
Angles	ω	Angles	ω	Angles	ω
N(1)—Co(1)—N(2)	111.09(19)	S(1)—C(1)—N(1)	178.9(5)	F(1)—C(7)—C(6)	113.9(5)
N(1)—Co(1)—N(1)#1	106.6(2)	S(2)—C(2)—N(2)	179.1(4)	F(1)—C(7)—C(8)	123.2(4)
N(1)—Co(1)—N(2)#1	109.44(18)	C(9)—P(1)—C(21)	107.5(2)	F(2)—C(3)—C(4)	115.0(5)
N(2)—Co(1)—N(2)#1	109.15(19)	C(9)—P(1)—C(27)	109.7(2)	F(2)—C(3)—C(8)	121.5(5)
Co(1)—N(1)—C(1)	170.6(5)	C(15)—P(1)—C(21)	108.2(2)	Br(1)—C(5)—C(4)	118.9(4)
Co(1)—N(2)—C(2)	178.0(4)	C(15)—P(1)—C(27)	113.5(2)	Br(1)—C(5)—C(6)	119.9(4)
C(9)—P(1)—C(15)	108.7(2)	C(21)—P(1)—C(27)	109.2(2)		

Symmetry transformations used to generate equivalent atoms: #1 $-x, y, 3/2-z$.

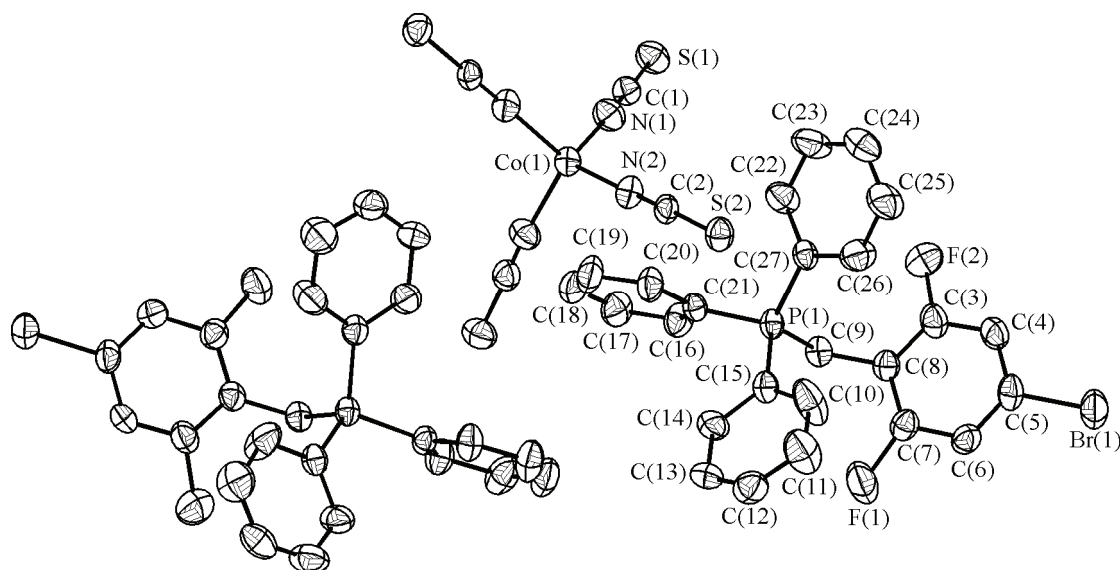


Fig. 1. ORTEP plot (30 % probability ellipsoids) showing the molecular structure of **1**

Results and discussion. In the IR spectra of **1**, for the cationic portion, the $\nu(\text{C—H})$ bands of methylene are seen at 2934 cm^{-1} , 2890 cm^{-1} . Bands at 1599 cm^{-1} , 1583 cm^{-1} , and 1481 cm^{-1} for **1** can be assigned to $\nu(\text{C=C})$ of the phenyl rings. The stretching bands of C—F and C—Br are at 1110 cm^{-1} and 529 cm^{-1} . For the anionic portions, the $\nu(\text{CN})$ and $\nu(\text{CS})$ stretching frequencies of KSCN are at 2053 cm^{-1} and 748 cm^{-1} ; when the N atom of the SCN ion is coordinated to the Co(II) ion, $\nu(\text{CN})$ and $\nu(\text{CS})$ are shifted to a higher frequency and they are 2077 cm^{-1} and 849 cm^{-1} for **1** [12]. The UV-Vis absorption spectra of **1** in HPLC grade CH_3CN ($1.0 \times 10^{-4}\text{ mol}\cdot\text{dm}^{-3}$) in the region of 200–900 nm are attributed to the anionic portions of these salts. The broad $d-d$ transition band is observed at 626 nm for **1**, while two CT bands can be observed at 319 nm and 269 nm for **1** [13]. The positive-ion ESI-MS spectrum of **1** in a CH_3CN solution shows that the mass spectra dominated by the peaks at 468.2 are assigned to $[\text{BiF}_4\text{BrBzTPP}]^+$. Molar conductivities of **1** at $1.0 \times 10^{-3}\text{ mol}\cdot\text{dm}^{-3}$ in a HPLC grade CH_3CN solution are $234.4\text{ S}\cdot\text{cm}^2\cdot\text{mol}^{-1}$, which indicate that the salt is 2:1 electrolyte [14].

$[\text{BiF}_4\text{BrBzTPP}]_2[\text{Co}(\text{NCS})_4]$ (**1**) crystallizes in the monoclinic crystal system, the space group $C2/c$, and an asymmetric unit in a cell comprises one $[\text{Co}(\text{NCS})_4]^{2-}$ anion and two $[\text{BiF}_4\text{BrBzTPP}]^+$ cations, as shown in Fig. 1. The selected bond distances and angles were listed in Table 1. For the $[\text{Co}(\text{NCS})_4]^{2-}$ anion, the coordination geometry of the central Co(II) ion could be described as a slightly distorted tetrahedron, and the average Co—N bond distance is 1.978 \AA , and the N—Co—N bond angles vary in the range $106.6\text{--}111.09^\circ$; these values are in agreement with those found in the complexes containing the $[\text{Co}(\text{NCS})_4]^{2-}$ anion [9, 15]. The $[\text{BiF}_4\text{BrBzTPP}]^+$ cation adopts a conformation in which four phenyl rings are twisted with respect to the C—C—P reference plane. The dihedral angles between the C(8)—C(9)—P(1) reference plane and the phenyl rings are 89.9° for the C(3)—C(8) ring, 108.2° for the C(10)—C(15) ring, 3.0° for the C(16)—C(21) ring, and 73.1° for the C(22)—C(27) ring. The most interesting fact is that $[\text{BiF}_4\text{BrBzTPP}]^+$ cations form a chain (Fig. 2) through $\text{F}\cdots\text{F}$ interactions with the distance of 3.224 \AA [16–19]. The chains of cations are linked through short $\text{F}\cdots\text{F}$ interactions. It is noted that two weak interactions are found in both anion and cation: (1) the short $\text{C}\cdots\text{Br}$ and $\text{N}\cdots\text{Br}$ interactions with the C(2) \cdots Br(1) and N(1) \cdots Br(1) distances of 3.613 \AA and 3.650 \AA (Fig. 3, a); (2) the C(12)—H(12) \cdots S(1ⁱ) ($i = 1/2-x, -1/2+y, 3/2-z$) hydrogen bonds with the distance of 2.926 \AA from H(12) to S(1ⁱ) (Fig. 3, b). These weak interactions consolidate the stacking of the molecules.

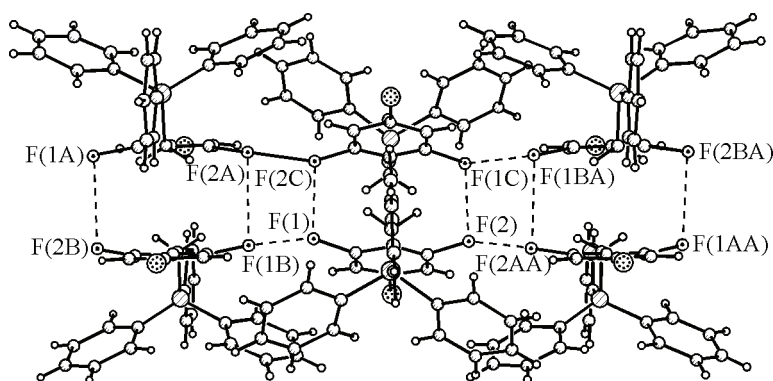


Fig. 2. Short F...F interactions between $[\text{BiF}_4\text{BrBzTPP}]^+$ cations for **1**

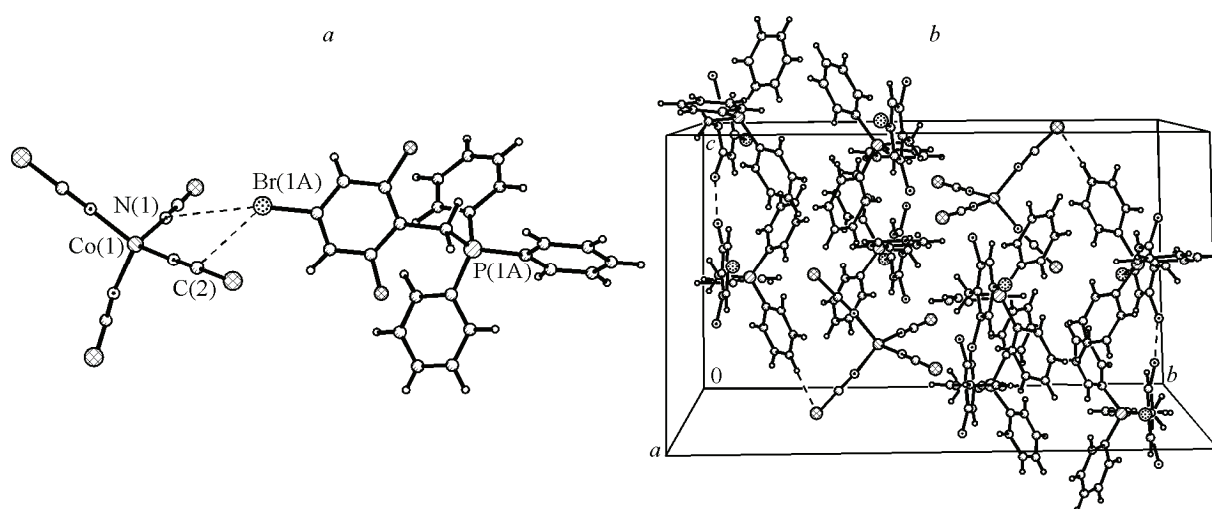


Fig. 3. (a) Short C...Br and N...Br interactions between the anions and cations for **1**; (b) weak C—H...S hydrogen bonds between the anions and cations for **1**

Magnetic properties. The crushed crystals of **1** are used to collect the variable-temperature (2—300 K) magnetic susceptibility data under a field of 2000 Oe. As shown in Fig. 4, the $\chi_M T$ value at 300 K is $2.054 \text{ emu} \cdot \text{K} \cdot \text{mol}^{-1}$, which is slightly larger than the spin-only value of high-spin Co(II) ($S = 3/2$) of $1.875 \text{ emu} \cdot \text{K} \cdot \text{mol}^{-1}$, indicating a contribution of the orbital momentum typical of the $^4T_{1g}$ ground state [20, 21]. As the temperature is lowered, the $\chi_M T$ product first smoothly decreases to $1.958 \text{ emu} \cdot \text{K} \cdot \text{mol}^{-1}$ around 20 K, then decreases sharply to reach a low value ($1.373 \text{ emu} \cdot \text{K} \cdot \text{mol}^{-1}$) at 2.0 K, indicative of the antiferromagnetic exchange. The

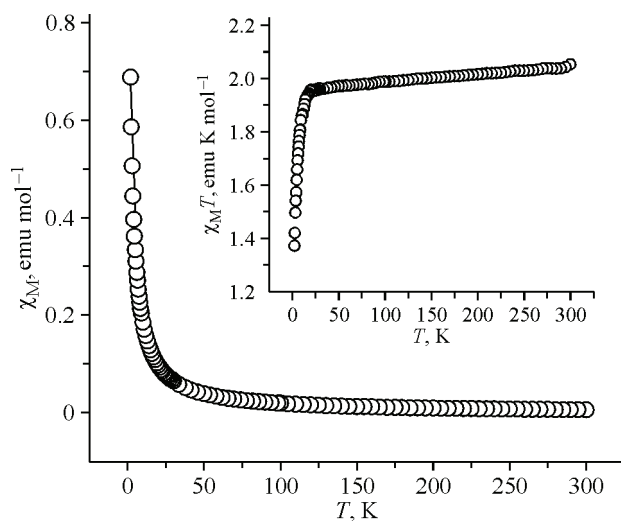


Fig. 4. Plot of χ_m versus T for **1** (inset: $\chi_m T$ versus T). The solid line is reproduced from the theoretical calculation and a detailed fitting procedure described in the text

temperature dependence of the susceptibility (χ_M) can be well fitted by the Curie-Weiss law with the fitting parameters being $C = 2.01 \text{ emu} \cdot \text{K} \cdot \text{mol}^{-1}$, $\theta = -0.977 \text{ K}$ and $R = 5.48 \times 10^{-6}$ (the solid line in Fig. 4).

This work has been supported by the Science and Technology Project (No. 2011B080701026, 2012B010200041) from Guangdong Science, the key Academic Program of the 3rd phase "211 Project" (No. 2009B010100001) of South China Agricultural University, the Guangdong Natural Science Foundation (No. 10151064201000022), and the university students' innovative training project (No. 10564112056, 201210564056) from Education Department of Guangdong Province.

REFERENCES

1. Ohba M., Okawa H. // *Coord. Chem. Rev.* – 2000. – **198**. – P. 313.
2. Minacheva L.K., Ivanova I.S., Tsivadze A.Y. et al. // *Russ. J. Inorg. Chem.* – 2002. – **47**. – P. 1301.
3. Noh T.H., Kim J.H., Lee Y.A. et al. // *J. Mol. Struct.* – 2003. – **691**. – P. 165.
4. Martin D.P., Knapp W.R., Supkowski R.M. et al. // *Inorg. Chim. Acta.* – 2009. – **362**. – P. 1559.
5. Ni C.L., Li Y.Z., Meng Q.J. // *J. Coord. Chem.* – 2005. – **58**. – P. 759.
6. Chen X., Yin W.T., Huang Q. et al. // *Transit. Met. Chem.* – 2010. – **35**. – P. 143.
7. Chen X., Lin J.H., Zhou H.L. et al. // *Inorg. Chim. Acta.* – 2010. – **363**. – P. 4024.
8. Zhou J.R., Ni C.L., Yu L.L. // *Inorg. Chim. Acta.* – 2008. – **361**. – P. 400.
9. Chen X., Chen W.Q., Han S. et al. // *J. Mol. Struct.* – 2010. – **984**. – P. 164.
10. Broos R., Anteunis M. // *Synth. Commun.* – 1976. – **6**. – P. 53.
11. Sheldrick G.M. SHELXTL, Bruker AXS Inc Madison, 1997.
12. Nakamoto K. *Infrared and Raman Spectra of Organic and Coordination Compounds*. 3rd Edition. – New York: Wiley, USA, 1978.
13. Banerjee S., Ray A., Sen S. et al. // *Inorg. Chim. Acta.* – 2008. – **361**. – P. 2692.
14. Geary W.J. // *Coord. Chem. Rev.* – 1971. – **7**. – P. 81.
15. Chen H.J., Zhang L.Z., Cai Z.G. et al. // *J. Chem. Soc., Dalton Trans.* – 2000. – P. 2463.
16. Baker R.J., Colavita P.E., Murphy D.M. et al. // *J. Phys. Chem.* – 2012. – **116**. – P. 1435.
17. Halper S.R., Cohen S.M. // *Inorg. Chem.* – 2005. – **44**. – P. 4139.
18. Barcelo-Oliver M., Estarellas C., Garcia-Raso A. et al. // *Crystengcomm.* – 2010. – **12**. – P. 3758.
19. Matta C.F., Castillo N., Boyd R.J. // *J. Phys. Chem.* – 2005. – **109**. – P. 3669.
20. Wei Y., Wu K., Broer R. et al. // *Inorg. Chem. Commun.* – 2007. – **10**. – P. 910.
21. Li B.L., Wang X.Y., Zhu X. et al. // *Polyhedron.* – 2007. – **26**. – P. 5219.